

DOI:10.1002/ejic.201301424

Luminescent AgAu Alloy Clusters Derived from Ag Nanoparticles – Manifestations of Tunable Au^I–Cu^I Metallophilic Interactions

Kumaranchira R. Krishnadas,^[a] Thumu Udayabhaskararao,^[a] Susobhan Choudhury,^[b] Nirmal Goswami,^[b] Samir Kumar Pal,^[b] and Thalappil Pradeep*^[a]

Keywords: Clusters / Nanoparticles / Luminescence / Closed-shell ions / Metallophilic interactions / Silver / Gold

Luminescent AgAu alloy quantum clusters are synthesized by a simple method that utilizes the galvanic reduction of polydisperse plasmonic silver nanoparticles. The clusters are characterized by ultraviolet–visible (UV/Vis) absorption spectroscopy, photoluminescence (PL) spectroscopy, X-ray photoelectron spectroscopy (XPS), transmission electron microscopy (TEM), and matrix-assisted laser desorption ionization mass spectrometry (MALDI MS). Selective and tunable quenching of cluster luminescence by Cu^{II} ions is observed and depends highly on the solvent as well as the protecting ligands. Metal-ion selectivity is exclusively caused by metallophilic interactions with the cluster core, and the tunability depends on the nature of the protecting ligands as well as

solvent effects. Detailed XPS and time-resolved luminescence measurements reveal that the tunability of luminescence quenching is achieved by the systematic variation of the metallophilic interactions between the Au^I ions of the alloy cluster and Cu^I ions formed by the reduction of Cu^{II} ions by the cluster core. This is the first report of tunable metallophilic interactions between monolayer-protected quantum clusters and a closed-shell metal ion. We hope that these results will draw more attention to the field of quantum cluster–metal ion interactions and provide useful insights into the stability of these clusters, origin of their intense luminescence, mechanisms of metal-ion sensing, and also help in the development of methods for tuning their properties.

Introduction

Inherent molecule-like properties and synergistic effects owing to the presence of heteroatoms make dimetallic quantum clusters fascinating materials in modern cluster science. Doping with other metals has been shown to enhance the chemical stability^[1] as well as tune the electronic structure of quantum clusters.^[2] The presence of a heteroatom in the core is expected to result in unusual chiroptical and magnetic properties in dimetallic clusters. Despite their promising applications, the synthesis of such dimetallic quantum clusters with atomically precise composition is a big challenge. Among these clusters, Au–Ag^[3] and Au–Pd^[4] systems are common systems, and Au–Cu,^[5] Au–Pt,^[6] and Ag–Ni^[7] clusters have also been reported. The simultaneous

reduction of individual precursors^[3–7] and galvanic reduction of presynthesized quantum clusters^[10,11] are some of the methods utilized for the synthesis of dimetallic quantum clusters. Although galvanic reduction is extensively utilized for the synthesis of dimetallic nanocrystals with controlled shapes and compositions,^[8] it is rarely utilized for the synthesis of atomically precise quantum clusters. Murray et al. have shown that it is possible to make dimetallic clusters from silver clusters^[9] by this method, and galvanic reduction has recently been utilized to synthesize atomically precise Ag–Au clusters from presynthesized thiolate-protected^[10] and protein-protected silver clusters.^[11]

The interaction of metal ions with quantum clusters is an active topic of research. Metal ions induce new chemical and electrochemical reactivities in clusters and modify their absorption and emission features. Muhammed et al.^[12a] reported the first metal-ion-induced changes in the optical properties of quantum clusters, and their reactivities with metal ions were investigated.^[12b] Quantum confinement in nanoparticles significantly alters their redox potentials^[13] and results in unexpected electrochemical reactions that cannot be explained by conventional electrochemistry.^[14] Although there are some previous investigations on the size-dependent changes in the reduction potential of metal clusters,^[15] the electrochemical reactivities of metal clusters remain largely unexplored. Metal-ion-induced changes in

[a] DST Unit of Nanoscience (DST UNS) and Thematic Unit of Excellence (TUE), Department of Chemistry, Indian Institute of Technology Madras, Chennai 600036, India
E-mail: pradeep@iitm.ac.in
www.dstuns.iitm.ac.in

[b] Department of Chemical Biological & Macromolecular Sciences, S. N. Bose National Centre for Basic Sciences, Block JD, Sector III, Salt Lake, Kolkata 700098, India

Supporting information for this article is available on the WWW under <http://dx.doi.org/10.1002/ejic.201301424>.

cluster luminescence has been extensively exploited for highly selective and sensitive detection of these species.^[16] The distinct roles of the inner core and ligand shells of these clusters and photophysical mechanisms behind these interactions have not been investigated in detail. Recently, metallophilic interactions between closed-shell metal ions with quantum dots^[17] and protein-protected Au clusters^[18] were shown to result in quenching of their luminescence. Metallophilic interactions, weak bonding interactions between two closed-shell metal ions, are a well-known phenomenon in Au^I complexes and heterometallic clusters of transition metals.^[19] However, this is not a well-recognized phenomenon in monolayer-protected noble-metal quantum clusters. Pyykko et al. presented the first theoretical studies on the interactions between a closed-shell Au_n cluster and closed-shell Au^I species.^[20] This work raised the possibility of metallophilic interactions between the inner Au_n core and Au^I ions in the protecting thiolate staple motifs of the clusters and is of immediate relevance to monolayer-protected quantum clusters. Explorations of such interactions in these systems may provide valuable insights into their stability, the origin of their intense luminescence, mechanisms of metal-ion sensing, and may also offer strategic methods for tuning their properties.

Here, we present the utility of the galvanic reduction reaction as a simple method for the synthesis of luminescent monodisperse AgAu quantum clusters protected by mercaptosuccinic acid (AgAu@MSA) derived from polydisperse plasmonic Ag nanoparticles (AgNPs). These clusters are synthesized at room temperature and no external reducing agent is required. The use of Ag nanoparticles as the precursor, instead of atomically precise Ag quantum clusters, makes the method more facile and scalable because of the inherent instability and difficult synthesis of the latter. The intense red luminescence of these clusters under UV irradiation and their high stability in aqueous solutions may make this material useful for biological applications. The luminescence of this cluster is selectively quenched by Cu^{II} ions. Detailed X-ray photoelectron spectroscopy (XPS) measurements show that Cu^{II} ions are reduced by interactions with the clusters. Even though Murray et al. and Wu et al. have shown that negatively charged as well as neutral Au₂₅ clusters can reduce more reactive metal ions such as Ag^I and Cu^{II} ions,^[14] no such reports exist on the redox reactivities of alloy clusters. Time-resolved as well as steady-state luminescence measurements show that this reactivity leads to metallophilic interactions between the Au^I ions of the clusters and Cu^I ions formed by the reduction of Cu^{II} ions by the clusters. Also, we report the solvent- and protecting-ligand-dependent tunability of these interactions, which are reflected in the changes in the luminescence of the cluster. Reports on such tunable metal-ion interactions with the clusters are scarce in the literature. This is the first report of tunable metallophilic interactions between monolayer-protected quantum clusters and a closed-shell metal ion. These metallophilic-interaction-induced changes in cluster luminescence are useful for the selective detection of Cu^{II} ions in water below permissible levels.^[16a]

Results and Discussion

Synthesis and Characterization of Alloy Clusters

AgAu@MSA clusters were synthesized by galvanic reduction of AgNPs by Au^I-MSA thiolates. Figure 1 shows the time-dependent changes in the UV/Vis features during the reaction. The plasmonic feature at 410 nm of AgNPs disappeared immediately after the addition of Au^I-MSA solution, and a new feature appeared at around 600 nm, which gradually disappeared and the spectrum became featureless. The solution was stirred for one hour and centrifuged subsequently to remove larger alloy nanoparticles and AgCl. The UV/Vis spectrum of the resuspended precipitate (Figure S1) showed a broad peak at ca. 600 nm, which is between the Au and Ag plasmonic peaks. This may be due to the formation of larger AgAu alloy nanoparticles. We propose that during the galvanic reduction, larger nanoparticles in the polydisperse AgNP sample react with Au^I-MSA to form larger AgAu dimetallic nanocrystals, and very small particles undergo galvanic reduction to form AgAu dimetallic quantum clusters (a schematic of the reaction is given in the inset of Figure 1). The TEM images shown in the inset of Figure 1 clearly show the decrease in the particle size from AgNPs to AgAu@MSA clusters. As the larger nanoparticles have lower solubility in methanol, these dimetallic nanoparticles precipitate, and the smaller dimetallic clusters remain in solution. The formation of AgCl was confirmed by XRD analyses of the precipitate (Figure S2).

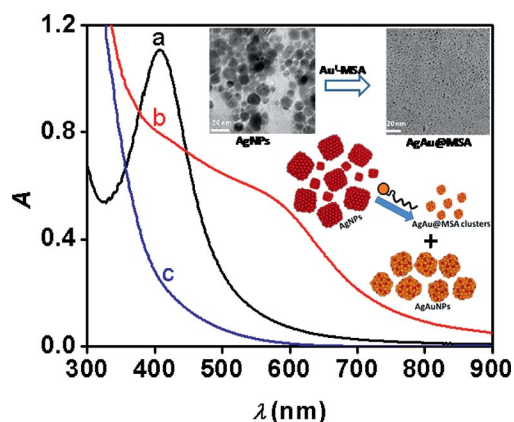


Figure 1. Time-dependent changes in the UV/Vis features during the reaction between AgNPs and Au^I-MSA thiolates in methanol. (a) UV/Vis spectra of AgNPs in methanol, (b) immediately after the addition of Au^I-MSA, and (c) after one hour of the reaction.

Insets a and a' in Figure 2 show the photographs of the precursor AgNPs under visible and UV light, respectively. Immediately after the addition of Au^I-MSA, this solution showed red emission under UV illumination. The time-dependent evolution of the luminescence features is shown in Figure S3, and typical luminescence features of the cluster are shown in Figure 2. The cluster showed a broad emission peak at 675 nm at 365 nm excitation. Insets b and b' of Figure 2 show the photographs of the AgAu@MSA cluster under visible and UV light, respectively.

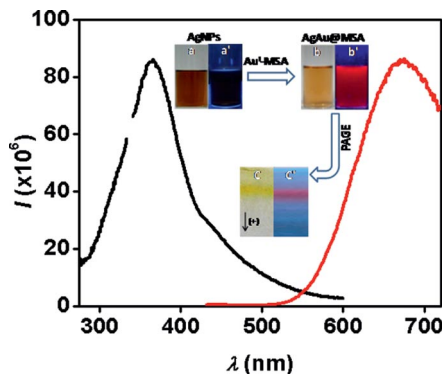


Figure 2. Excitation and emission spectra of AgAu@MSA clusters in methanol. The insets are the photographs of (a and a') the AgNP solution, (b and b') the AgAu@MSA solution, and (c and c') the PAGE-separated clusters under visible and UV light, respectively. The discontinuity in the excitation peak shows the position at which the secondary of the emission maximum appears.

Polyacrylamide gel electrophoresis (PAGE) was performed to check the purity of the as-synthesized clusters (details in the Supporting Information). The inset photographs (c and c') of Figure 2 show the presence of a single band of the gel after PAGE separation. The band appeared light yellow under visible light and bright red under a UV lamp. This shows that monodisperse dimetallic clusters can be synthesized from polydisperse plasmonic silver nanoparticles by using the galvanic reduction method.

The XPS survey spectrum shown in Figure 3 (a) indicates the presence of all expected elements. The Au 4f_{7/2} peak at 84.1 eV shows that the Au atoms are in the zero oxidation state. The Ag 3d_{5/2} peak at 368.0 eV^[10] indicates the presence of metallic Ag in the cluster. The S 2p_{3/2} peak at 162.2 eV suggests that sulfur is attached to the metal core in the form of thiolate.^[22] Energy-dispersive X-ray analysis (EDAX) also confirmed the presence of the constituent elements in the cluster (Figure S4).

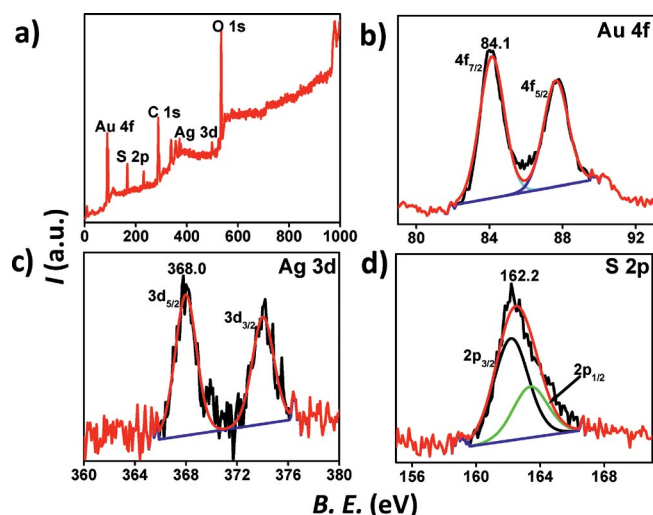


Figure 3. (a) XPS survey spectrum of the AgAu@MSA cluster and expanded regions of it showing the (b) Au 4f, (c) Ag 3d, and (d) S 2p features.

Figure 4 shows the matrix-assisted laser desorption ionization mass spectra (MALDI MS) of the clusters after ligand exchange with hexanethiol. Ligand exchange was attempted because MSA-protected clusters do not give intact ions in MALDI MS. This is also the case with glutathione-protected clusters.^[23] The inset of Figure 4 shows the luminescence spectral features of the cluster before (in water) and after (in toluene) ligand exchange. The excitation maximum of the cluster shows a blueshift of ca. 20 nm after ligand exchange, and the emission maximum is blueshifted by ca. 5 nm. These shifts could be caused by the difference in the polarities of water and toluene. The excitation and emission spectral shapes are preserved after ligand exchange, which shows that the composition of the cluster core is unchanged. At the threshold laser fluence, a peak at 17 kDa appears, and the peak shifts to the lower mass region owing to fragmentation of the cluster upon increasing laser fluence.

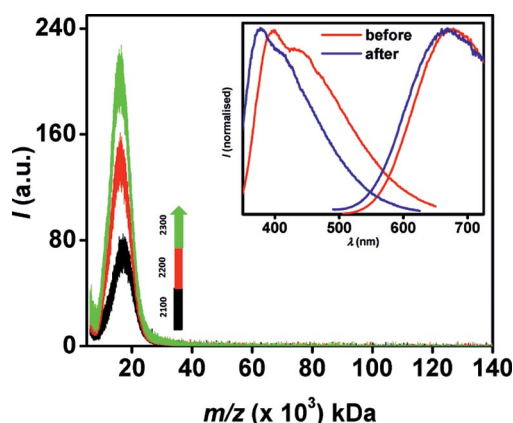


Figure 4. Laser-intensity-dependent MALDI MS spectra of the AgAu clusters, ligand-exchanged with hexanethiol. The numbers by the side of the arrow indicate the laser intensity as given by the instrument. The inset shows the excitation and emission spectra of the cluster before and after ligand exchange.

Tunable Interactions of the Alloy Clusters with Cu^{II} Ions

Interactions of metal ions with the quantum clusters affect their absorption and emission features. Metal-ion-induced luminescence changes of quantum clusters were utilized extensively for the selective detection of trace quantities of metal ions.^[16,24] To study the interaction of metal ions with the AgAu@MSA clusters, the luminescence spectra of these clusters were measured in the presence of various metal ions. Aqueous solutions of various metal ions (100 μL, 100 ppm) were added to the cluster solution in methanol. The luminescence of the AgAu@MSA clusters was quenched immediately after the addition of a Cu^{II} solution. Figure 5 (a) shows that quenching is selective to Cu^{II} ions, and there is no significant decrease in luminescence intensity upon the addition of other metal ions. The addition of Cu^{II} ions resulted in gradual precipitation of the clusters from the solution. These observations may invoke the possibility of aggregation-induced luminescence

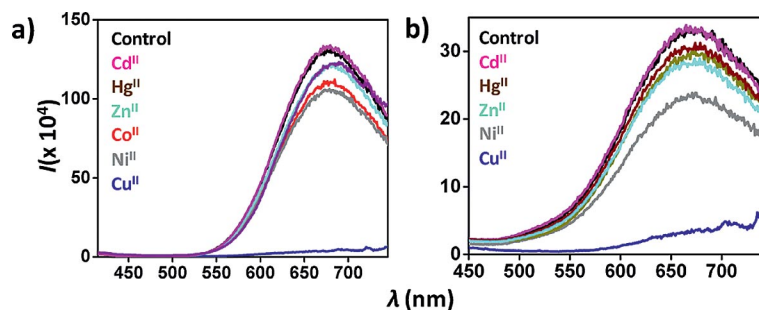


Figure 5. Emission spectra of (a) AgAu@MSA clusters in methanol and (b) AgAu@BBS clusters in THF in the presence of various metal ions.

quenching, resulting from the binding of Cu^{II} ions to the carboxylate groups of the MSA ligands, which was suggested as a metal-ion-induced quenching mechanism in noble-metal clusters.^[24] Aggregation-induced quenching occurs by the reabsorption of the emitted radiation from the fluorophore, and for this phenomenon to be feasible, the Stokes shift of the fluorophore should be very small. The large Stokes shift (ca. 310 nm) of the AgAu@MSA cluster also suggests that this phenomenon is not likely. The UV/Vis absorption spectrum of the cluster was featureless, and no new features were observed after treatment with the Cu^{II} salt (Figure S5). Moreover, aggregation induced by the Cu^{II} ions should not affect the cluster core and, hence, the binding energies of the core atoms will not be shifted. XPS measurements (Figure 8) show that the Au binding energy is shifted to higher values. This evidence clearly indicates the absence of aggregation-induced quenching.

To determine whether the observed metal-ion selectivity is due to the specific interaction of Cu^{II} ions with the core or the carboxylate groups of the ligand shell of the AgAu cluster, quenching experiments were performed with clusters that had been ligand-exchanged with *tert*-butylbenzyl mercaptan (BBSH). As the sulfur atom of this ligand is bound to the AgAu core of the cluster and there are no other functional groups such as $-\text{COOH}$, the possibility of ligand- Cu^{II} interactions is eliminated. Interestingly, the luminescence of the ligand-exchanged cluster (AgAu@BBS) was also quenched by Cu^{II} ions (Figure 5, b), that is, the selectivity towards Cu^{II} ions was retained even after ligand exchange. These observations clearly suggest that the origin of metal-ion selectivity is the interaction of Cu^{II} ions with the AgAu core of the cluster.

The addition of oxalic acid (OA) into the Cu^{II} -treated AgAu@MSA solution in methanol (solution 1) resulted in complete recovery of the luminescence (Figure 6, a). This shows that the interaction of Cu^{II} ions with the clusters is almost completely reversible in methanol. As oxalic acid is a very strong chelator for Cu^{II} ions, it forms stable copper oxalate, which results in the recovery of the luminescence. The addition of Cu^{II} ions into a mixture of OA and the clusters did not result in any quenching (Figure S6); this shows that OA effectively prevents cluster- Cu^{II} interactions. Interestingly, the luminescence of a AgAu@BBS- Cu^{II} mixture in tetrahydrofuran (THF; solution 3) was not at all

recovered by the addition of OA (Figure 6, c). To check the role of change in solvent from methanol to THF on the observed irreversibility, quenching experiments were performed with AgAu@MSA clusters in THF. Interestingly,

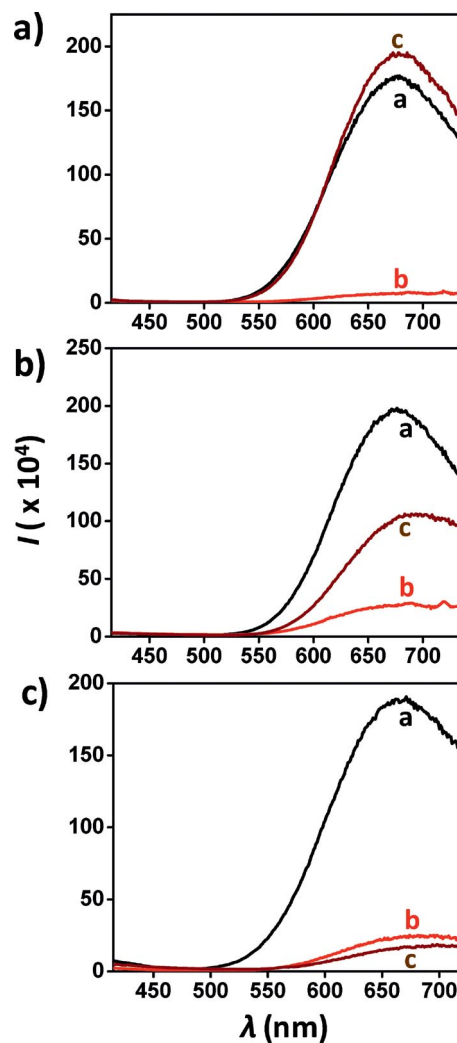


Figure 6. Emission spectra of (a) AgAu@MSA clusters in methanol and (b) THF and (c) AgAu@BBS clusters in THF showing the changes in luminescence upon the addition of Cu^{II} ions and OA. In each panel, traces a–c corresponds to the pure cluster, the cluster with Cu^{II} ions, and the cluster with Cu^{II} ions and OA, respectively.

we observed a partial recovery (Figure 6, b) of the luminescence upon the addition of OA into a AgAu@MSA-Cu^{II} mixture in THF (solution 2). This indicates that in addition to the solvent, the nature of the protecting ligand is also important in the determination of the reversibility of the interaction (see below for possible effects of solvent and protecting ligands). These observations show that the cluster-Cu^{II} interactions that lead to luminescence quenching are tunable with respect to the solvent and the nature of the protecting ligand. However, we observed a redshift of the emission maximum (ca. 5 nm for solution 1 and ca. 10 nm for solutions 2 and 3) upon the addition of Cu^{II} ions, and the shift was retained even after the addition of OA.

XPS measurements of the Cu^{II}-treated clusters (Figure 7) show that the Cu 2p_{3/2} peak is shifted to lower binding energies compared to that of metallic Cu (935.5 eV). Cu^{II} shows a well defined peak shape with characteristic satellite structure. The presence of Cu 2p features in all the treated samples indicates that Cu is part of the samples. Note that the XPS sample preparation involves washing the sample. However, complete absence of the satellite structure in these samples suggests reduction of the Cu^{II} ions. For solution 1, the Cu 2p_{3/2} peak is at 932.5 eV, whereas for solutions 2 and 3, these peaks are shifted to 932.3 and 932.2 eV, respectively. As the difference in the Cu^I and Cu⁰ binding energies is only ca. 0.1–0.2 eV,^[25] it is difficult to assign the exact Cu oxidation states in the mixtures. However, the reduction of Cu^{II} to Cu^I/Cu⁰ is evident from these measurements. The characteristic ligand-to-metal charge-transfer satellite of Cu^{II} at 946 eV is absent in the treated samples, indicating the complete absence of the Cu^{II} state in the samples.

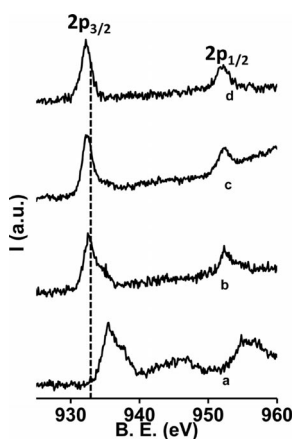


Figure 7. Cu 2p regions in the X-ray photoelectron spectra of pure and Cu^{II}-treated AgAu clusters. Traces a–d correspond to CuSO₄ and solutions 1, 2, and 3, respectively.

Figure 8 shows the Au 4f binding energies for the pure and Cu^{II}-treated clusters. The Au 4f_{7/2} peak for the pure AgAu@MSA cluster is at 84.1 eV. For solutions 1 and 2, this peak is shifted to 84.6 eV. This peak shifts further to 85.0 eV for solution 3. The binding energies for Ag were almost unchanged for the pure as well as Cu^{II}-treated clusters (Figure S7). This clearly indicates that the Cu^{II} ions interact preferentially with the Au atoms of the alloy cluster.

Elemental analysis (Figure S4) shows that the alloy cluster is mostly composed of Au. Galvanic reduction by Au^I thiolates is initiated on the surface of the AgNPs, and most of the Ag atoms will be released as Ag^I ions and a few Ag atoms will be entrapped by Au atoms. Hence, these Ag atoms are more likely to be in the inner core of the cluster, which make them inaccessible to the Cu^{II} ions. This could be the reason for the preferential interaction of the Cu^{II} ions with the Au atoms of the cluster.

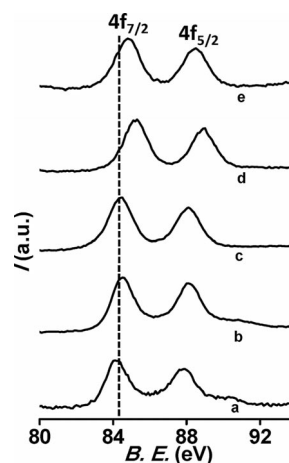


Figure 8. Au 4f region in the X-ray photoelectron spectra of pure and Cu^{II}-treated AgAu clusters. Traces a–e correspond to pure AgAu@MSA and solutions 1–4, respectively.

Notably, the observed trend in reversibility of the luminescence parallels the changes in the Au 4f_{7/2} binding energies. The Au 4f_{7/2} peak for solutions 1 and 2 (for which the luminescence was completely and partially reversible, respectively) is at 84.6 eV, which is between those for the pure clusters (84.1 eV) and AgAu@BBS (85.0 eV). The shift in the Au 4f_{7/2} peak (from 84.1 to 85.0 eV) is maximum for solution 3, for which irreversible quenching of luminescence was observed.

We suggest that the clusters can undergo two kinds of interactions with Cu^{II} ions. XPS measurements clearly indicate that the Cu^{II} ions are reduced as a result of their interactions with the cluster. The decrease in Cu binding energy (to that of Cu^I/Cu⁰) and increase in that of Au in the clusters may be an indication of a redox reaction between the cluster core and Cu^{II} ions (reaction 1). The redshift of the emission maximum of the clusters after treatment with Cu^{II} ions could be an indication of the oxidation of the clusters. The reduction of the Cu^{II} ions by a noble metal such as Au may seem contradictory when considering the conventional electrochemical potentials. It is to be noted that the standard electrochemical potentials in the literature are those of bulk electrodes. In the case of nanoparticles, especially at the quantum cluster regime, electrochemical potentials will be very much determined by quantum confinement effects. A few earlier investigations^[15c,15d] on small metal clusters have shown that their reduction potentials were lower than the bulk values. Hence, at the cluster regime, these types of redox processes are feasible. Another possibility for the reduction of the Cu^{II} ions is the replacement of some of the

Au^I ions of the thiolate staple motifs by Cu^{II} ions, which may lead to the formation of a mixed thiolate shell containing both Au^I and Cu^I ions (reaction 2). This leads to the reduction of Cu^{II} to Cu^I as in the case of copper thiolates.^[26] We could not confirm this interaction by an analysis of the S 2p binding energies of the samples as there were no significant changes in the S 2p binding energies of solutions 1 and 2, compared to that of pure clusters. Notably, the S 2p binding energies of copper and gold thiolates are almost the same (ca. 162 eV).^[22,26] However, for solution 3, the S 2p_{3/2} binding energy was 162.7 eV (data not shown), which is higher than that of the pure clusters (162.2 eV). XPS of the OA-treated solution 1 (solution 4; sample for which luminescence was completely recovered) indicates that the Au 4f binding energies remain at higher values (84.6 eV). This shows that the clusters undergo an irreversible oxidation as a result of their interactions with the Cu^{II} ions (reaction 1). Reaction 2 is expected to result in complete reversibility of the Au 4f binding energies to those of the pure clusters after treatment with OA, as all of the Cu^I ions are completely removed by OA. Once the Cu^I ions have been removed by OA, the Au^I ions can bind with the ligands (released from Cu^I), and this will regenerate the pure clusters and should lead to the reversal of the Au 4f binding energies to that of the pure clusters. However, this reversal of binding energies was not observed. These observations indicate that reaction 1, that is, the galvanic reduction, is the most likely interaction between the clusters and Cu^{II} ions.

To understand the mechanism of the observed fluorescence quenching of AgAu@MSA clusters in presence of Cu^{II} ions, we plotted (Figure 9) the fractional fluorescence according to the Stern–Volmer Equation (1).

$$\frac{F_0}{F} = 1 + K_D[Q] \quad (1)$$

F_0 and F are the fluorescence intensity in the absence and presence of quencher, respectively, $[Q]$ is the concentration of quencher and K_D is the Stern–Volmer quenching con-

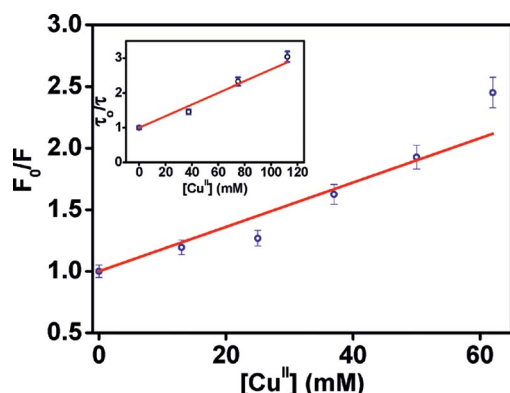


Figure 9. Stern–Volmer plot for the luminescence quenching of AgAu@MSA clusters in methanol upon the addition of Cu^{II} ions. The inset shows the change of τ_0/τ_{av} with Cu^{II} ion concentration.

stant. From Figure 9, we have found a linear response of fluorescence as a function of Cu^{II} ion concentration. This result indicates that the nature of quenching is dynamic.

Picosecond time-resolved luminescence measurement is a useful technique to aid understanding of the photophysical processes behind the observed quenching of the AgAu@MSA clusters. A gradual and significant decrease in the average lifetime (Figure S8 and Table S1) with increasing quencher concentration indicates the occurrence of dynamic quenching. The plot of τ_0/τ_{av} against Cu^{II} concentration (inset of Figure 9) was linear, as expected for a dynamic quenching process. The decay profiles for pure clusters and solution 1 are shown in Figure 10. The decay transients are fitted tri-exponentially, and the fitting parameters are tabulated in Table 1. Similar decay behaviors were also observed for solutions 2 and 3 (Tables S2 and S3, Figure S9 and S10, respectively). The decay profiles indicate the dynamic nature of quenching for all cases.

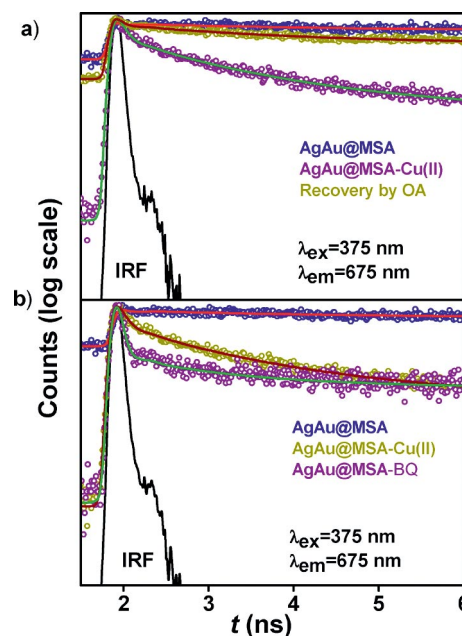


Figure 10. Picosecond time-resolved fluorescence transients of AgAu@MSA clusters in methanol. (a) The quenching of luminescence lifetime upon the addition of Cu^{II} ions and its recovery upon the addition of OA and (b) upon the addition of Cu^{II} ions and benzoquinone.

Table 1. Picosecond time-resolved luminescence transients of AgAu@MSA before and after the treatment with Cu^{II} and recovery by OA in methanol. AgAu@MSA was also treated with BQ.

System	τ_1 [ns] (%)	τ_2 [ns] (%)	τ_3 [ns] (%)	τ_{av} [ns]
Pure AgAu@MSA cluster in methanol	0.16 (38)	1.12 (20)	50 (42)	21.3
Cluster with Cu ^{II}	0.10 (65)	1.24 (22)	12 (13)	1.93
Cluster with OA	0.09 (52)	1.64 (20)	50 (28)	14.4
Cluster with BQ	0.07 (71)	1.58 (9)	55 (20)	11.2

Dynamic quenching can occur through various processes such as Förster resonance energy transfer (FRET) and photoinduced electron transfer (PET). However, the absence of

any permanent oscillating dipole (owing to the acceptor) rules out the possibility of a FRET process. The absence of an electron transfer processes is further confirmed by control experiments with benzoquinone (BQ), a well-known electron acceptor. In presence of BQ, an ultrafast time component (70 ps) evolves with very sharp decay with a contribution of 71% (Figure 10, b). No such drastic changes in the ultrafast components are observed for the Cu^{II}-treated samples, which rules out the possibility of an ultrafast PET process from the cluster to the Cu^{II} ions. This is supported by measurements at different Cu^{II} ion concentrations, for which the gradual reduction of the longer time component was observed with minor alteration of the shorter time constant (Figure S8 and Table S1).

Similar lifetime decay patterns were reported for Au₂₅@BSA clusters upon the interaction with Hg^{II} ions.^[18a] This was attributed to metallophilic bond-induced quenching of the delayed fluorescence. The observations of the reduction of the Cu^{II} ions along with the similarity in the decay patterns of the AgAu clusters strongly suggest the possibility of metallophilic interactions. We suggest the following mechanism for the observed selective and tunable quenching interactions. The Cu^{II} ions are first reduced to Cu^I by a redox reaction with the AgAu core of the cluster (reaction 1). The 3d¹⁰ orbital of the Cu^I ions and the 5d¹⁰ orbital of either the Au^I ions of the thiolate staple motifs or the Au atoms of the partially oxidized cluster take part in metallophilic interactions. As the staple motifs have a significant role in the electronic structure of monolayer-protected clusters,^[27] these interactions can lead to changes in the electronic structure and to quenching. Metallophilic interactions between Au^I and Cu^I ions are recognized both theoretically and experimentally in diverse systems and have been utilized in applications such as vapochromic sensors.^[28] We suggest that galvanic reduction-induced metallophilic interactions are the key factor that determines the selectivity towards metal ions. Among the metal ions tested, only the Cu^{II} and Hg^{II} systems possess positive reduction potentials and, hence, these ions can be reduced most easily by the quantum clusters. The reduction potentials of the other metal ions are negative and, hence, they cannot be reduced by these clusters. In addition to the electrochemical potentials, the requirement of a closed-shell electronic configuration for metallophilic interactions immediately reveals the reason behind the observed metal-ion selectivity. Among Cu^{II} and Hg^{II}, only Cu^{II} can attain a closed-shell configuration (of Cu^I) from core-induced reduction, and this might be the reason behind the observed selectivity towards Cu^{II}. Even though Hg^{II} can be reduced to Hg^I by the cluster, this reduction will lead to the formation of an ion without a closed-shell configuration. Notably, the addition of Hg^{II} ions to the clusters does not lead to any immediate luminescence quenching. However, quenching owing to the addition of Hg^{II} ions was observable only after about 5 h (data not shown). Earlier studies on the reaction of quantum clusters with Hg^{II} ions show that the Hg^{II} ions were reduced mostly to Hg^I and not to Hg⁰.^[12b] This could

be due to the high affinity of mercury towards the thiolate ligands of the cluster.

We suggest that solvents as well as protecting ligands play a crucial role in the tunability of the luminescence quenching of these AgAu clusters. Solvents can induce structural changes in the cluster core as well as the thiolate staple motifs. Recent studies on Au–Cu clusters protected by alkynyl ligands^[29a] show that solvents can induce structural reorganization of clusters by affecting the strength of metallophilic bonding, and this leads to changes in the luminescence features. Studies on Au^I thiolates have shown that solvents can induce Au^I–Au^I metallophilic interactions caused by aggregation and lead to visible photoluminescence.^[29b] These solvent effects will modulate the strength of Au^I–Cu^I bonding in these clusters and lead to tunable quenching interactions. As mentioned earlier, changes in the bonding of thiolate staple motifs alter the electronic structure of clusters, which in turn affects the luminescence features of the cluster.^[27]

Metallophilic bonding can originate from different types of interactions between the closed-shell species such as van der Waals, ionic, and charge-transfer forces. Theoretical studies on Au^I–Cu^I metallophilic bonds^[28a] show that this bond is mainly due to ionic forces between the two species. Hence, changes in the solvent polarity are expected to significantly affect the nature of this bond. As the polarity of the solvent decreases, the ionic-interaction-based metallophilic bond becomes less feasible and the bond becomes more covalent in nature and, hence, stronger. Therefore, the Au^I–Cu^I bond will be weaker (i.e., this bond will be only metallophilic in nature) in a polar solvent such as methanol than in THF. The efficient chelation of Cu^I species happens in methanol and in turn results in complete recovery of the luminescence. The complete recovery of luminescence was further confirmed by experiments with the clusters in acetone as another polar solvent (Figure S11). We also observe the recovery in the time-resolved measurements (see Figure 10, a). In THF, the metallophilic contributions to the Au^I–Cu^I bond will be less, and the covalent nature of the bond increases. This makes the Au^I–Cu^I bond stronger and, hence, chelation with OA will be less facile. This could be the reason for the partial recovery of luminescence for the AgAu@MSA clusters in THF. Note that the dielectric constants of methanol, acetone, and THF are 33, 21, and 7.5, respectively. However, we could not demonstrate the irreversible quenching for the MSA-protected sample in a solvent less polar than THF because of the insolubility of the clusters and Cu^{II} salts in such solvents. In the case of the ligand-exchanged clusters, the Au^I–Cu^I bond experiences a much more nonpolar environment (owing to the BBSH or hexanethiol ligand shell) compared to the case with the AgAu@MSA clusters in THF. Therefore, the Au^I–Cu^I bond will be strongest for the ligand-exchanged cluster in THF. In this case, the chelation of the Cu^I ions with OA will be least facile. This could be the reason behind the irreversible quenching of the ligand-exchanged cluster. The selectivity towards Cu^{II} ions and irreversibility of the lumi-

nescence quenching are further confirmed with clusters that are ligand-exchanged with hexanethiol.

To check the practical utility of these interactions for Cu^{II} detection, the luminescence intensities of aqueous solutions of AgAu@MSA with different Cu^{II} concentrations (in parts per million) were measured (Figure 11). A good linear response of the materials towards Cu^{II} ions was observed. From this plot, the detection limit is 0.5 ppm, which is well below the permissible limit of Cu^{II} ions in water (1.3 ppm). As the reduction potentials of the clusters depend on their composition, we expect that these interactions can be utilized for ultra-low-level detection with clusters of varied composition, which can be easily synthesized by our method.

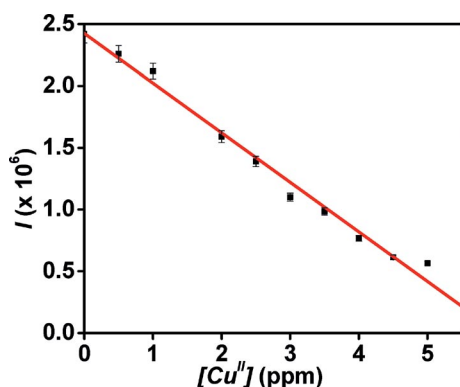


Figure 11. Variation of the luminescence intensity of the AgAu@MSA clusters in water with concentration of Cu^{II} ions, immediately after the addition.

Conclusions

Luminescent AgAu dimetallic quantum clusters were synthesized by a simple method that utilizes the galvanic reduction of polydisperse plasmonic nanoparticles. The clusters were characterized by various spectroscopic and microscopic tools. The luminescence of the clusters is selectively quenched by Cu^{II} ions, and the quenching is highly tunable depending on the solvent and the ligand used. Detailed XPS measurements indicate that the clusters undergo a redox reaction with Cu^{II} ions. Steady-state as well as time-resolved luminescence measurements prove that the tunability is due to the galvanic reduction-induced tunable metallophilic interactions between the Au^I ions of the cluster and Cu^I ions formed by the reduction of Cu^{II} ions by the cluster. This is the first report of tunable metallophilic interactions between monolayer-protected quantum clusters and a closed-shell metal ion. We hope that our results draw more attention to the chemistry of quantum clusters with metal ions in general and the metallophilic interactions of clusters in particular.

Experimental Section

Materials: Chloroauric acid (HAuCl₄·3H₂O), mercaptosuccinic acid (MSA), and 4-*tert*-butylbenzyl mercaptan (BBSH) were pur-

chased from Sigma–Aldrich. Silver nitrate and tetrahydrofuran (THF) were purchased from RANKEM. Hexanethiol was purchased from Fluka. Oxalic acid, CuSO₄·5H₂O, CdCl₂, ZnSO₄, HgCl₂, NiCl₂, and Co(OAc)₂ were purchased from Merck. All chemicals were used without any further purification.

AgAu@MSA Clusters: MSA-protected AgNPs were synthesized by following a reported procedure.^[21] A stock solution was prepared by dissolving purified AgNPs (80 mg) in distilled water (10 mL). Au^I MSA thiolate was prepared in distilled water by dissolving MSA powder (8.5 mg) in aqueous HAuCl₄ solution (5 mL, 5 mM). All reactions were performed at room temperature. For the synthesis of the AgAu@MSA clusters, the stock AgNP solution (0.5 mL) was diluted with methanol (to 10 mL). Au^I-MSA solution (2 mL) was added into the methanolic AgNP solution with stirring. The reaction was monitored by time-dependent UV/Vis absorption and photoluminescence measurements. Larger AgAu alloy nanoparticles and AgCl were removed by ultracentrifugation, and AgAu@MSA clusters were obtained as a clear solution in methanol. This solution was concentrated by rotary evaporation and then freeze-dried to afford a pasty material; excess thiolates prevented the production of clean powders from the system. Ethyl acetate was added to this pasty material to precipitate the pure AgAu@MSA, which was then collected and dried in nitrogen to afford dry powder samples.

Ligand Exchange of AgAu@MSA Clusters: The ligand (BBSH or hexanethiol) was dissolved in methanol (70 μL in 2 mL). This solution was added to AgAu@MSA cluster solution (2 mL) in distilled water, and the mixture was stirred at room temperature for 2 min. Toluene (4 mL) was then added, and the mixture was stirred further for 3 min at room temperature. The aqueous layer became colorless, and the toluene layer became light yellow indicating the completion of the ligand exchange. The toluene layer was separated to afford a clear solution of ligand-exchanged AgAu cluster.

Instrumentation: UV/Vis absorption spectra were recorded with a Perkin–Elmer Lambda 25 instrument in the spectral range 200–1100 nm. Transmission electron microscopy (TEM) of the samples was performed by using a JEOL 3010 instrument with an ultrahigh resolution (UHR) polepiece. TEM specimens were prepared by drop-casting one or two drops of the aqueous solution to carbon-coated copper grids and allowed to dry at room temperature overnight. All measurements were performed at 200 kV to minimize the damage of the sample by the high-energy electron beam. X-ray photoelectron spectroscopy (XPS) measurements were performed with an Omicron ESCA Probe spectrometer with polychromatic Mg-K_α X-rays (*hν* = 1253.6 eV). The X-ray power applied was 300 W. The pass energy was 50 eV for survey scans and 20 eV for specific regions. Sample solutions were spotted on a molybdenum sample plate and dried in vacuo. The base pressure of the instrument was 5.0 × 10⁻¹⁰ mbar. The binding energy was calibrated with respect to the adventitious C 1s feature at 285.0 eV. Deconvolution of the spectra was performed by using the CASAXPS software. Matrix-assisted laser desorption/ionization mass spectrometry (MALDI MS) studies were conducted with a Voyager-DE PRO Biospectrometry Workstation from Applied Biosystems. A pulsed nitrogen laser of 337 nm was used for the MALDI MS studies. The samples were mixed with a *trans*-2-[3-(4-*tert*-butylphenyl)-2-methyl-2-propenyldiene]malononitrile (DCTB) matrix in 1:1 ratio, spotted on the target plate, and allowed to dry under ambient conditions. Mass spectra were collected in the negative-ion mode and were averaged for 200 shots. Scanning electron microscopy (SEM) and energy-dispersive X-ray (EDAX) analysis were performed with an FEI QUANTA-200 SEM. For measurements, samples were drop-

casted on an indium tin oxide coated conducting glass and dried in ambient conditions. Picosecond-resolved fluorescence decay transients were measured and fitted by using a commercially available spectrophotometer (Life Spec-ps, Edinburgh Instruments, UK) with an 80 ps instrument response function (IRF).

Supporting Information (see footnote on the first page of this article): Procedure for the PAGE experiment, UV/Vis spectra of the product and byproducts, XRD pattern of the AgCl formed as a byproduct, time-dependent evolution of the photoluminescence of the clusters during the reactions, EDAX spectrum and elemental composition of the cluster, UV/Vis spectra of the cluster in methanol with and without Cu^{II} ions, emission spectra of AgAu@MSA in methanol containing oxalic acid and its stability of fluorescence upon the addition of Cu^{II} ions, Ag 3d regions in the X-ray photoelectron spectra of pure and Cu^{II}-treated AgAu@MSA clusters, lifetime measurements of alloy clusters containing different Cu^{II} concentrations, lifetime decay profiles and fitting parameters for solutions 2 and 3, luminescence data showing the complete reversibility of the quenching in acetone.

Acknowledgments

The authors thank the Department of Science and Technology (DST), New Delhi, Government of India, for constantly supporting our research programme on nanomaterials. S. K. P. thanks the DST for financial grants (DST/TM/SERI/2k11/103 and SB/S1/PC-011/2013). Mr. M. S. Bootharaju is thanked for the assistance in XPS measurements. K. R. K. thanks the University Grants Commission (UGC), New Delhi for a research fellowship. N. G. and S. C. thank the Council of Scientific and Industrial Research (CSIR), New Delhi for fellowships.

- [1] Y. Negishi, K. Igarashi, K. Munakata, W. Ohgake, K. Nobusada, *Chem. Commun.* **2012**, 48, 660–662.
- [2] Y. Negishi, T. Iwai, *Chem. Commun.* **2010**, 46, 4713–4715.
- [3] C. Kumara, A. Dass, *Nanoscale* **2011**, 3, 3064–3067.
- [4] a) Y. Negishi, W. Kurashige, Y. Niihori, T. Iwasa, K. Nobusada, *Phys. Chem. Chem. Phys.* **2010**, 12, 6219–6225; b) S. Xie, H. Tsunoyama, W. Kurashige, Y. Negishi, T. Tsukuda, *ACS Catal.* **2012**, 2, 1519–1523.
- [5] Y. Negishi, K. Munakata, W. Ohgake, K. Nobusada, *J. Phys. Chem. Lett.* **2012**, 3, 2209–2214.
- [6] H. Qian, D. Jiang, G. Li, C. Gayathri, A. Das, R. R. Gil, R. Jin, *J. Am. Chem. Soc.* **2012**, 134, 16159–16162.
- [7] S. R. Biltek, S. Mandal, A. Sen, A. C. Reber, A. F. Pedicini, S. N. Khanna, *J. Am. Chem. Soc.* **2013**, 135, 26–29.
- [8] a) S. Xie, M. Jin, J. Tao, Y. Wang, Z. Xie, Y. Zhu, Y. Xia, *Chem. Eur. J.* **2012**, 18, 14974–14980; b) H. Zhang, M. Jin, J. Wang, W. Li, P. H. C. Camargo, M. J. Kim, D. Yang, Z. Xie, Y. Xia, *J. Am. Chem. Soc.* **2011**, 133, 6078–6089; c) W. Zhang, J. Yang, X. Lu, *ACS Nano* **2012**, 6, 7397–7405.
- [9] T. Huang, R. W. Murray, *J. Phys. Chem. B* **2003**, 107, 7434–7440.
- [10] T. U. B. Rao, Y. Sun, N. Goswami, S. K. Pal, K. Balasubramanian, T. Pradeep, *Angew. Chem.* **2012**, 124, 2197; *Angew. Chem. Int. Ed.* **2012**, 51, 2155–2159.
- [11] J. S. Mohanty, P. L. Xavier, K. Chaudhari, M. S. Bootharaju, N. Goswami, S. K. Pal, T. Pradeep, *Nanoscale* **2012**, 4, 4255–4262.
- [12] a) M. A. H. Muhammed, T. Pradeep, *Chem. Phys. Lett.* **2007**, 449, 186–190; b) M. S. Bootharaju, T. Pradeep, *Langmuir* **2011**, 27, 8134–8143.
- [13] P. Hoyer, H. Weller, *Chem. Phys. Lett.* **1994**, 221, 379–384.
- [14] a) J.-P. Choi, C. A. Fields-Zinna, R. L. Stiles, R. Balasubramanian, A. D. Douglas, M. C. Crowe, R. W. Murray, *J. Phys. Chem. C* **2010**, 114, 15890–15896; b) Z. Wu, *Angew. Chem.* **2012**, 124, 2988; *Angew. Chem. Int. Ed.* **2012**, 51, 2934–2938.
- [15] a) A. Henglein, *J. Phys. Chem.* **1993**, 97, 5457–5471; b) J. Belloni, *Catal. Today* **2006**, 113, 141–156; c) K. Mallick, Z. L. Wang, T. Pal, *J. Photochem. Photobiol. A: Chem.* **2001**, 140, 75–80; d) H. Remita, S. Remita, in: *Recent Trends in Radiation Chemistry* (Eds.: J. F. Wishart, B. S. M. Rao), World Scientific Publishing Co. Pte. Ltd., Singapore, **2010**, chapter 13.
- [16] a) Y. Guo, Z. Wang, H. Shao, X. Jiang, *Analyst* **2012**, 137, 301–304; b) M. A. H. Muhammed, P. K. Verma, S. K. Pal, A. Retnakumari, M. Koyakutty, S. Nair, T. Pradeep, *Chem. Eur. J.* **2010**, 16, 10103–10112; c) I. Chakraborty, T. Udayabhaskararao, T. Pradeep, *J. Hazard. Mater.* **2012**, 211–212, 396–403; d) G.-Y. Lan, C.-C. Huang, H. T. Chang, *Chem. Commun.* **2010**, 46, 1257–1259; e) B. Adhikari, A. Banerjee, *Chem. Mater.* **2010**, 22, 4364–4371; f) H. Liu, X. Zhang, X. Wu, L. Jiang, C. Burda, J. J. Zhu, *Chem. Commun.* **2010**, 47, 4237–4239; g) A. George, E. S. Shibu, S. M. Maliyekkal, M. S. Bootharaju, T. Pradeep, *ACS Appl. Mater. Interfaces* **2012**, 4, 639–644; h) Y.-T. Su, G.-Y. Lan, W.-Y. Chen, H.-T. Chang, *Anal. Chem.* **2010**, 82, 8566–8572; i) N. Goswami, A. Giri, M. S. Bootharaju, P. L. Xavier, T. Pradeep, S. K. Pal, *Anal. Chem.* **2011**, 83, 9676–9680; j) E. S. Shibu, T. Pradeep, *Chem. Mater.* **2011**, 23, 989–999.
- [17] N. Goswami, A. Giri, S. Kar, M. S. Bootharaju, R. John, P. L. Xavier, T. Pradeep, S. K. Pal, *Small* **2012**, 8, 3175–3184.
- [18] a) P. Yu, X. Wen, Y.-R. Toh, J. Huang, J. Tang, *Part. Part. Syst. Charact.* **2013**, 30, 467–472; b) J. Xie, Y. Zheng, J. Y. Ying, *Chem. Commun.* **2010**, 46, 961–963.
- [19] a) H. Schmidbaur, S. Cronje, B. Djordjevic, O. Schuster, *Chem. Phys.* **2005**, 311, 151–161; b) P. Pyykko, *Chem. Rev.* **1988**, 88, 563–594; c) S. Sculfort, P. Braunstein, *Chem. Soc. Rev.* **2011**, 40, 2741–2760; d) H. Schmidbaur, A. Schier, *Chem. Soc. Rev.* **2008**, 37, 1931–1951.
- [20] P. Pyykko, X.-G. Xiong, J. Li, *J. Chem. Soc., Faraday Discuss.* **2011**, 152, 169–178.
- [21] T. Udayabhaskararao, T. Pradeep, *Angew. Chem.* **2010**, 122, 4017; *Angew. Chem. Int. Ed.* **2010**, 49, 3925–3929.
- [22] M. S. Bootharaju, G. K. Deepesh, T. Udayabhaskararao, T. Pradeep, *J. Mater. Chem. A* **2013**, 1, 611.
- [23] E. S. Shibu, B. Radha, P. K. Verma, P. Bhyrappa, G. U. Kulkarni, S. K. Pal, T. Pradeep, *ACS Appl. Mater. Interfaces* **2009**, 1, 2199–2210.
- [24] a) C.-C. Huang, Z. Yang, K. H. Lee, H. T. Chang, *Angew. Chem.* **2007**, 119, 6948; *Angew. Chem. Int. Ed.* **2007**, 46, 6824–6828; b) W. Chen, X. Tu, X. Guo, *Chem. Commun.* **2009**, 1736–1738.
- [25] Z. Ai, L. Zhang, S. Lee, W. Ho, *J. Phys. Chem. C* **2009**, 113, 20896–20902.
- [26] N. Sandhyarani, T. Pradeep, *J. Mater. Chem.* **2001**, 11, 1294–1299.
- [27] Z. Wu, R. Jin, *Nano Lett.* **2010**, 10, 2568–2573.
- [28] a) M. Rodriguez-Castillo, M. Monge, J. M. Lopez-de-Luzuriaga, M. E. Olmos, A. Laguna, F. Mendizabal, *Comput. Theor. Chem.* **2011**, 965, 163–167; b) S. Tsukamoto, S. Sakaki, *Dalton Trans.* **2013**, 42, 4809; c) E. Strasser, V. J. Catalano, *J. Am. Chem. Soc.* **2010**, 132, 10009–10011.
- [29] a) I. O. Koshevoy, Y. C. Chang, A. J. Karttunen, M. Haukka, T. Pakkanen, P.-T. Chou, *J. Am. Chem. Soc.* **2012**, 134, 6564–6567; b) Z. Luo, X. Yuan, Y. Yu, Q. Zhang, D. T. Leong, J. Y. Lee, *J. Am. Chem. Soc.* **2012**, 134, 16662–16670.

Received: November 7, 2013

Published Online: December 13, 2013